Soft Matter

Frustration between two- and three-dimensional smectic ordering leads to a biaxial nematic phase

Journal:	*Soft Matter*
Manuscript ID	SM-ART-09-2019-001809.R1
Article Type:	Paper
Date Submitted by the Author:	12-Nov-2019

Complete List of Authors:	Chen, Dong; Zhejiang University, Institute of Process Equipment, College of Energy Engineering; Zhejiang University, State Key Laboratory of Fluid Power and Mechatronic Systems; University of Colorado Boulder, Physics Department and Soft Materials Research Center Coleman, David; University of Colorado Boulder, Physics Department and Soft Materials Research Center Zhu, Chenhui; Lawrence Berkeley National Laboratory; University of Colorado Boulder, Physics Department and Soft Materials Research Center Chattham, Nattaporn; Kasetsart University, Physics Department; University of Colorado Boulder, Physics Department and Soft Materials Research Center Jenz, Frank; University of Stuttgart, Institute of Physical Chemistry; University of Colorado Boulder, Physics Department and Soft Materials Research Center Cheng, Xiaohong; Yunnan University, Department of Chemistry, Key Laboratory of Medicinal Chemistry for Natural Resources; Martin-Luther-Universitat Halle-Wittenberg, Institute of Organic Chemistry Tschierske, Carsten; Martin-Luther-Universitat Halle-Wittenberg, Institute of Organic Chemistry Glaser, Matthew; University of Colorado Boulder, Physics Department and Soft Materials Research Center Maclennan, Joseph; University of Colorado Boulder, Physics Department and Soft Materials Research Center Clark, Noel; University of Colorado Boulder, Physics Department and Soft Materials Research Center

Frustration between two- and three-dimensional smectic ordering leads to a biaxial nematic phase

Dong Chen,[a,b,c] David A. Coleman,[c] Chenhui Zhu,[c] Nattaporn Chattham,[c,d] Frank Jenz,[c,e] Xiaohong Cheng,[f,g] Carsten Tschierske,[f] Matthew A. Glaser,[c] Joseph E. Maclennan,[c] and Noel A. Clark[c*]

[a]Institute of Process Equipment, College of Energy Engineering, Zhejiang University, Zheda Road No.38, Hangzhou, 310027, China

[b]State Key Laboratory of Fluid Power and Mechatronic Systems, Zhejiang University, Zheda Road No. 38, Hangzhou, 310027, China

[c]Department of Physics and Soft Materials Research Center, University of Colorado, Boulder, CO 80309-0390, USA

[d]Department of Physics, Faculty of Science, Kasetsart University, Bangkok, 10900, Thailand

[e]Institute of Physical Chemistry, University of Stuttgart, D-70569 Stuttgart, Germany

[f]Institute of Organic Chemistry, Martin-Luther-University, D-06108, Halle, Germany

[g]Department of Chemistry, Key Laboratory of Medicinal Chemistry for Natural Resources, Yunnan University, Kunming, Yunnan 650091, China

*Email: Noel.Clark@colorado.edu

Abstract

The bola-amphiphilic, T-shaped mesogen CT2 has an aromatic biphenyl core terminated on both ends by hydrophilic groups and a semi-perfluorinated aliphatic side chain. Upon cooling from the isotropic phase, the fluorinated tails and the polar, rod-like cores nanophase-segregate to form a fluid lamellar phase. At high temperatures, the biphenyl cores are orientationally disordered in two dimensions (2D) in the lamellar planes but on further cooling the cores order orientationally, giving a biaxial lamellar phase with 2D nematic in-plane ordering. At lower temperature, the aromatic and hydrophilic parts of the cores nanosegregate within the lamellae and 2D smectic correlations of the head groups develop. X-ray diffraction shows that this 2D smectic ordering is incompatible with the initial lamellar structure, with both structures becoming short-ranged, resulting in a 3D biaxial nematic phase with macroscopic orthorhombic symmetry featuring strong smectic correlations in two orthogonal spatial dimensions. Freeze-fracture transmission electron microscopy enables direct visualization of the resulting short-ranged periodic structures.

Introduction

The introduction of strong polyphilicity into the molecular structure of liquid crystal-forming molecules has expanded opportunities for the creation of new phases and liquid crystal materials based on the tiling of space with domains of distinct chemical functionality [1, 2, 3, 4]. In these phases, aromatic cores functionalized with two or more chemically incompatible side chains or tails form the boundaries in tiled columnar phases, the structure of which is established by a strong tendency for nanosegregation and judicious choice of molecular sub-volumes and geometry [4]. While these features can be successfully employed in the directed design of some spectacular new phases, they also lead to the possibility of novel frustration effects if molecular geometry and the relative volumes of the molecular sub-components are not sufficiently compatible with an optimal solution to filling space and competing chemical segregation tendencies are strong. We report high-resolution, synchrotron x-ray diffraction (XRD) and freeze-fracture transmission electron microscopic (FFTEM) studies of the phase phenomenology of a T-shaped polyphilic mesogen, CT2, one of a number of bola-amphiphiles designed and synthesized by the Tschierske group [5, 6, 7, 8]. Lamellar smectic ordering appears via a first-order phase transition upon cooling from the high temperature isotropic phase as a result of the nanophase segregation of aromatic and fluoro-alkyl molecular subgroups, but is then suppressed upon further cooling by the distinct in-plane nanosegregation of aromatic and hydrophilic moieties.

The lamellar ordering enables the spreading of freely suspended films of CT2 as thin as two molecular layers, in which the phase sequence of in-plane 2D isotropic (2D–Iso or Lam-Iso), in-plane 2D nematic (2D–Nem or Lam-Nem) and in-plane 2D smectic (2D–Sm or Lam-Sm) has been studied by depolarized reflection microscopy [9]. Thin films of CT2 are particularly interesting, because dimensionality plays an important role in the formation of the liquid crystal phases. Theoretical treatments of nematic and smectic order and their transitions in two dimensions predict: *i)* While nematic order in 3D is inherently stable, nematic order in 2D is at its lower critical dimensionality ($d_{cNem} = 2$), becoming unstable at accessible temperatures against the spontaneous dissociation of topological point

singularities via the Kosterlitz-Thouless transition [2,10], and exhibiting a local mean-square difference in the orientation at different locations that increases logarithmically with separation [11], as is observed in the azimuthal orientation of molecular tilt (the "c-director" field) in smectic C films [12]; *ii)* The lower critical dimensionality for smectic layer ordering is $d_{cSm} = 3$, so that smectic layering in 2D is below its lower critical dimensionality and is therefore strictly short-ranged [5,13], unstable against the proliferation of in-plane edge dislocations, and exhibiting a $1/s$ divergence of the local relative mean-square layer displacement with average separation, s. The optical experiments on freely suspended bola-amphiphile films of thickness between 2 and 11 layers showed a nearly second-order Lam-Iso to Lam-Nem transition with the order parameter increasing continuously on cooling, and a continuous appearance of 2D smectic ordering at lower temperatures. The birefringence of the in-layer nematic and smectic textures in the thin films is substantially larger than that observed in bulk preparations [14, 15], indicating that the film geometry may substantially stabilize the layer structure by forcing the cores to be more parallel to the planes than they are in the bulk. Here we show that in the bulk, the in-plane smectic ordering appears discontinuously on cooling and, in doing so, disorders the already established 3D lamellar structure, leading to a low temperature phase that is nematic and biaxial.

Results

The chemical structure and phase sequence of CT2 are shown in Figure 1a. This remarkable mesogen exhibits both layering of the side chains (the “lamellae”) and additional in-plane 2D isotropic (Lam-Iso, Figure 1b), nematic (Lam-Nem, Figure 1c) and smectic (Lam-Sm, Figure 1d) ordering of the rigid molecular cores (head groups). We investigated the microstructures of these phases using FFTEM, a technique in which the structure of liquid crystal phases can be visualized directly [16]. Consistent with previous studies, in the Lam-Iso phase, the lamellae appear to have long-range positional order. The FFTEM images (Figure 2a) show flat lamellae with occasional steps in the topography, while the head

groups (not resolved in the FFTEM image) are disordered. On cooling, the rod-like molecular cores align along some average direction, forming the Lam-Nem phase. FFTEM images of the Lam-Nem phase (Figure 2b, magnified in Figure 2c and sketched in Figure 2d) are similar to Lam-Iso, showing smooth, featureless lamellae that are flat over long distances.

In the Lam-Sm phase, shown in Figure 3, FFTEM images reveal both lamellar structure, as evidenced by large, flat regions separated by steps (Figure 3a), and a modulated texture reflecting the in-plane positional and orientational ordering of the in-plane smectic layers (Figure 3c). In contrast to B1 and columnar phases, which are inherently stable in three dimensions and have in-plane ordering that is long-ranged and very regular (see Figures S1a-c and S2a-c, Supplementary Information), in the Lam-Sm phase, the 2D smectic order is only short-ranged (Figure 3b). The nanoscale texture shows a dislocated pattern of white stripes with a period of ~5 nm (Figure 3b) and, at higher magnification, dark bands perpendicular to these stripes with the periodicity *d* of the in-layer, head-group smectic (Figure 3c). In the FFTEM images, the smectic layers are interrupted by the white stripes but appear to be in register on either side of any given stripe and have the same orientation, suggesting that the stripes may just be an artefact of the fracturing process. However, since these stripes are generally oriented perpendicular to the smectic layers, we can use the distribution of stripe orientations as a means of estimating the in-layer smectic orientational ordering. As we shall see below, the smectic layer normal fluctuates around the local average direction and has orientational order comparable to that of a nematic. This picture is reminiscent of a model for smectic ordering proposed by Toner and Nelson [5,13], who noted that the effect of fluctuations and free dislocations is to destroy smectic order at length scales larger than the dislocation correlation length, limiting the smectic order to finite "blobs". The layering from blob to blob is not correlated in this model, and there is some variation in the direction of the layer normal across any given small area. On large length scales, the blobs constitute a nematic-like phase, with the director defined as the average layer normal of all the blobs.

Taking the white stripes to be a probe of the local in-layer orientation, the orientational order parameter of the 2D smectic phase of CT2 can be estimated by Fourier transforming an FFTEM image of one of the lamellae (Figure 3d), with a typical result shown in Figure 3e. The peaks corresponding to the first-order diffraction of the stripes are orientationally diffuse, indicative of short-range orientational correlations of the smectic layers as expected for Toner and Nelson's nematic-like smectic blob phase. The crescent-shaped scattering peaks due to the variation of the stripe orientation across the sample strongly resemble the familiar wide-angle x-ray scattering arcs of the nematic phase of rod-like molecules at wide angle. The contrast of the intensity modulations corresponding to the in-plane smectic layers in the FFTEM image is too small to yield an identifiable diffraction peak in the Fourier transform image. Nevertheless, the orientational order parameter of the stripes, and hence of the 2D layer normal, can be extracted from the scattering pattern as follows: First, the FWHM of the stripe diffraction peak, indicated approximately by the red circles in Figure 3e, is determined by analyzing the radial intensity profile (see Figure S3, Supplementary Information). The scattered intensity is then integrated radially over the width of the FWHM to obtain the average scattering from the layers as a function of azimuthal angle φ (see Figure S4, Supplementary Information). After redefining the origin of the azimuthal angle ϕ such that $\int I(\varphi)\sin\varphi d\varphi = 0$, we obtain two scattering peaks centered around ϕ=0 (Figure 3f), from which we can compute the 2D orientational order parameter, $S_2 = \ < \cos 2\varphi > = 0.84$. The order parameter of the smectic blobs is thus similar in magnitude to that of a conventional nematic phase formed by rod-like molecules [11].

Synchrotron-based powder x-ray scattering on bulk capillary samples using a four-circle diffractometer provided further insight into the nature of the lamellar and in-plane ordering in the Lam-Sm temperature range (140ºC < T < 152ºC). Two reflections are observed at small angle, one at $q_t \sim 0.18$ Å^{-1} (corresponding to a periodicity t ~ 34 Å) which is associated with the lamellar ordering, and one at $q_d \sim 0.32$ Å^{-1} (corresponding to a periodicity d ~ 20 Å) associated with the in-plane smectic ordering. The

distance of 20 Å corresponds to the length of antiparallel, fully intercalated pairs of molecules arranged parallel to the layer planes (see Fig. S5). The lamellar peak exhibits a strong temperature dependence, with the peak becoming broader, decreasing in height, and moving to smaller q with decreasing temperature (Figure 4a), while the scattering from the in-plane smectic layers is essentially independent of temperature (Figure 4b). These peaks were fit to Voigt lineshape functions and deconvolved from the resolution function (an example is shown in Figure 4c), assuming that the intrinsic lineshape is Lorentzian, to obtain the peak positions, q_t and q_d, integrated areas A_t and A_d, and spatial coherence lengths ξ_t and ξ_d as a function of temperature, shown in Figures 5a–c. This analysis reveals some striking features, indicative of bulk CT2 behavior that is quite different from that found in freely suspended films [19].

The lamellar peak appears upon cooling at T = 163ºC, with $q_t \sim 0.18$ Å^{-1} and a width only slightly exceeding the diffractometer resolution, giving correlation lengths $\xi_t \sim 8{,}000 - 10{,}000$ Å (corresponding to about 260 lamellae) over the temperature range 163ºC > T > 152ºC (Figure 5a). This is comparable to values measured in random focal conic textures of fluid smectics in capillaries, indicating long-range ordering of the lamellae in the Lam-Iso and Lam-Nem phases. On further cooling, however, this lamellar peak begins to broaden dramatically as can be seen in Figure 4a. This change of behavior coincides with the abrupt appearance, at T = 152ºC, of the in-plane reflection at $q_d \sim 0.32$ Å^{-1} (Figure 5b), indicative of a first-order Lam-Nem to Lam-Sm transition. The in-plane smectic reflection peak is significantly broader than the spectrometer resolution (Figure 4b), giving smectic correlation lengths ξ_d in the 3,000–4,000 Å range, corresponding to about 175 layers. Once this peak grows in, its shape remains essentially unchanged on cooling. The lamellar ordering is compromised by the appearance of in-plane smectic ordering in the Lam-Sm phase and both are short-ranged, the lamellar coherence length in the Lam-Sm phase being only $\xi_t = 630$ Å (about 20 lamellae) at T = 140ºC.

The lamellar correlation length $\xi_t(T)$ and peak area $A_t(T)$ have similar temperature dependence in the Lam-Sm phase, as seen from the inset of Figure 6a, which shows that they are approximately

proportional. Such a linear relation between A and ξ is familiar from the description of critical behavior, specifically the divergence of the q-space susceptibility $\chi(q) \propto I(q)$, the intensity of scattering by order parameter fluctuations on approaching a second-order phase transition [17]. Thus $\chi(\delta q) = \chi_o(T)\ \{1 + [\delta q \xi(T)]^2\}^{-1}$, where the susceptibility $\chi_o(T) \propto (T-T_c)^{-\gamma}$ is the peak value of $\chi(\delta q)$. The correlation length varies with temperature as $\xi(T) \propto (T-T_c)^{\nu}$ and δq measures the magnitude of q deviations from the mean layering wavevector q_t. Generally, for the growth of smectic correlations in nematics we have $\gamma \sim 2\nu$ [18], giving $\chi_o(T) \propto \xi(T)^2$ and thus $A(T) \propto \xi(T)$, since $A(T) \propto \chi_o(T)/\xi(T)$. If $A_t(T) \propto \xi_t(T)$ is the case for the lamellar reflection, the tails of the $I(\delta q_t)$ peaks should overlap at large δq_t (see [19], for example), which, as Figure 6 shows, is a feature of the peak growth in CT2.

The log-log plot of $I(\delta q_t)$ vs δq_t in Figure 6b indicates that the tails of the diffuse lamellar reflection peaks fall off with increasing δq_t as $I(\delta q_t) \sim 1/\delta q_t^2$, justifying the assumption made in the fitting that the intrinsic lineshapes are Lorentzian. When the lineshapes $I(\delta q_t)$ from a powder-averaged liquid crystal sample with short-range smectic layer correlations are Lorentzian, this indicates that the lineshape being orientationally powder averaged is locally Lorentzian-squared [19]. This, in turn, indicates that the layer correlations are limited by the presence of quenched, random forces **F(r)** acting on the layered system [19,20]. In this case, the Lorentzian local susceptibility $\chi(\delta q_t) = \chi_o(T)\ \{1 + [\delta q_t \xi_t(T)]^2\}^{-1}$ generates a local, single-domain scattering function (before powder averaging) of the form $I(\delta q_t) \propto \Delta_q[\chi(\delta q_t)^2] \propto \chi_o(T)^2\{1 + [\delta q_t \xi_t(T)]^2\}^{-2}$, where the prefactor Δ_q is proportional to the mean square value of **F** and is assumed not to depend on temperature [19]. The XRD measurements of CT2 indicate a susceptibility for lamellar ordering that diverges with decreasing temperature in the Lam-Sm phase, with the disordering fluctuations driven by quenched disorder.

The manifestation of a second smectic ordering in a pre-existing lamellar phase bears some resemblance to a kind of sliding phase [21] found in a DNA-lipid system where a lattice of DNA chains

(with in-plane order) is intercalated between bilayers of a lamellar lipid phase [22]. In this system, the DNA ordering is found to be short-ranged relative to that of the bilayer lamellae [23]. This is consistent with the fact that smectic layering in 2D is below its lower critical dimensionality and is unstable at accessible temperatures against the spontaneous dissociation of topological point singularities via the Kosterlitz-Thouless transition [2,10]. In CT2, on cooling through the Lam-Sm phase, the lamellar reflection moves to smaller q and broadens, the correlation length decreasing to ~630 Å (about 20 lamellae), appearing to be responding to a decreasing susceptibility for the lamellar ordering at lower temperature, and, as noted above, a disordering influence on the lamellar packing beyond thermal fluctuations. This disordering is a frustration effect coming from additional packing constraints imposed on the lamellae driven by enthalpy when the in-plane smectic order appears. This is directly confirmed by the orientational correlation of the in-plane smectic ordering from one lamella to another, as shown in Figure 7a and sketched in Figure 7b.

The resulting geometrically frustrated LC phase, being biaxial and nematic-like, could be considered as a special kind of cybotactic nematic phase with strong smectic correlations in two orthogonal spatial dimensions. This allows the local biaxiality to be manifested at a macroscopic level, resulting in the previously unobserved case of a spontaneously biaxial, thermotropic nematic phase with orthorhombic (D_{2h}) symmetry [24] that is stable even in the absence of external ordering forces.

Summary

The structures of the Lam-Iso, Lam-Nem and Lam-Sm phases of a T-shaped liquid crystal molecule, where the lateral chains (“tails”) form conventional lamellae and the aromatic cores (“heads”) arrange successively on cooling with in-plane isotropic, nematic and smectic ordering, have been visualized directly using freeze-fracture transmission electron microscopy. When the in-plane order is isotropic or nematic, the lamellar phase gives synchrotron Bragg scattering that is resolution-limited, indicating quasi-long-range or long-range ordering of the lamellae. When the in-plane order becomes

smectic, the spatial correlation of the 2D smectic layering imposes additional packing constraints on the system that render the lamellar order only short-ranged, an effect observed for the first time in a 3D system.

Acknowledgements

This work was supported by the Soft Materials Research Center under NSF MRSEC Grants DMR-0820579 and DMR-1420736. Use of the National Synchrotron Light Source was supported by the U.S. Department of Energy, Divisions of Materials and Chemical Sciences. D.C. was supported by the National Natural Science Foundation of China (Grants No. 11704331 and 21878258) and by the Fundamental Research Funds for the Central Universities (2018QNA4046).

Author Contributions

D.C., D.A.C., C.Z. and N.C. acquired data. D.C., F.J., M.A.G. and N.A.C. analysed the data. X.C. and C.T. synthesized the liquid crystal material. D.C., C.T., J.E.M. and N.A.C. wrote and edited the manuscript.

Additional Information

Competing financial interests: The authors declare no competing financial interests.

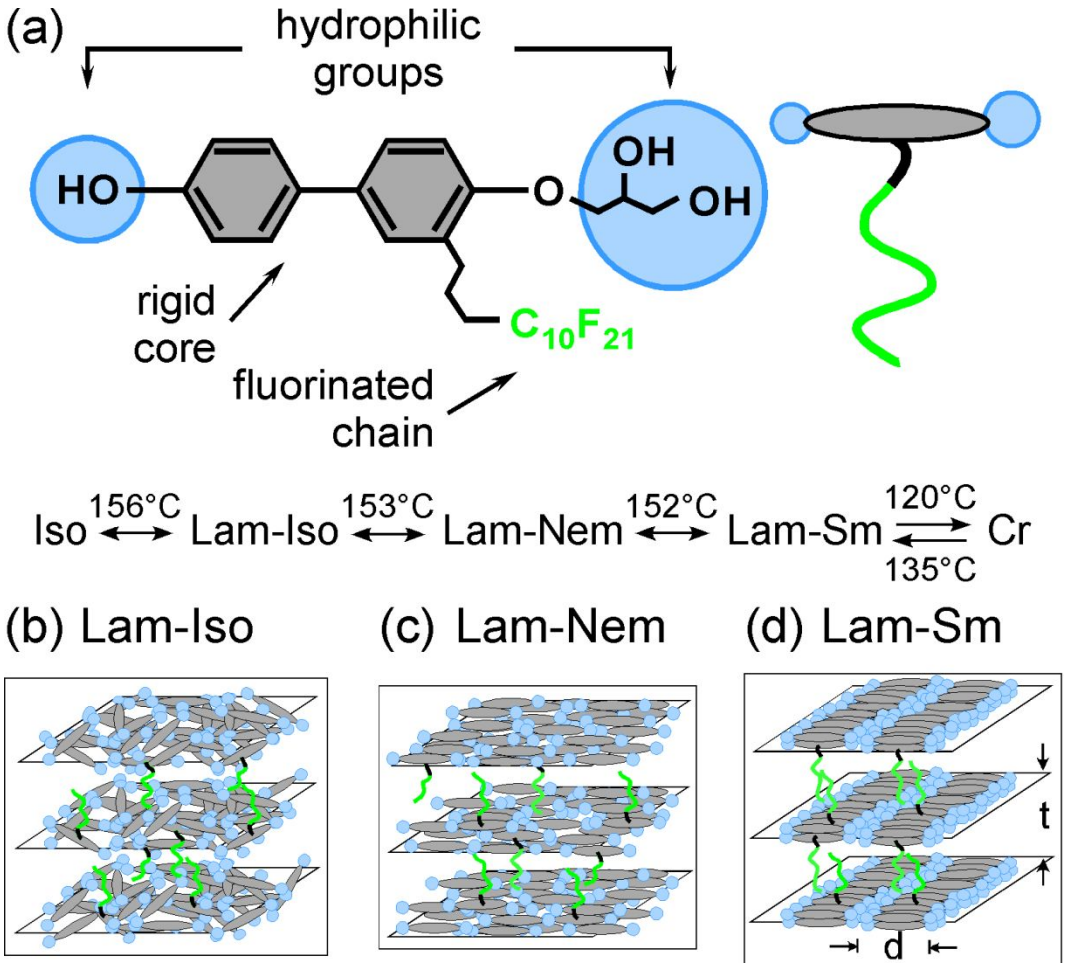

Figure 1: Structure and phases of the T-shaped bolaamphiphile, CT2. (a) Molecular structure and schematic drawing of mesogen, with phase sequence and transition temperatures shown for the bulk. The fluorinated tails (green) form a lamellar structure, with the rod-like molecular cores/head groups (gray) ordering in nanosegregated sheets. On cooling from the isotropic, CT2 forms lamellar phases that initially have no in-plane order (b) but develop nematic (c) and then smectic order (d) of the head groups in two dimensions. In the interests of clarity, orientational fluctuations are not shown in all schematics of the 2D nematic and smectic phases.

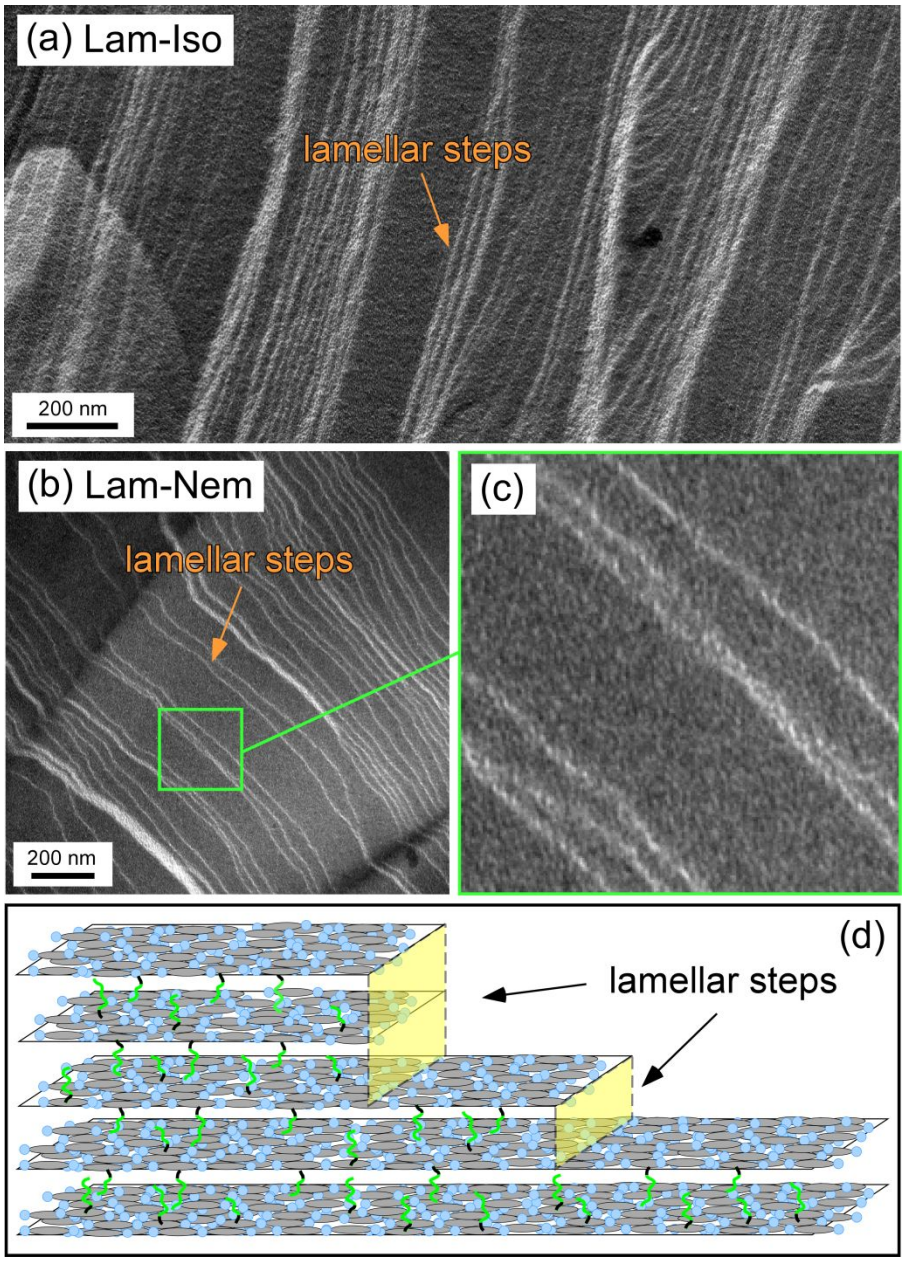

Figure 2: Microstructures of the Lam-Iso and Lam-Nem phases. (a) FFTEM image of the Lam-Iso phase quenched at 160ºC, showing smooth lamellae separated by steps. There are no identifiable in-plane features. (b) FFTEM image of the Lam-Nem phase fractured in the bulk. No particular in-plane texture can be distinguished, even when magnified as in (c). Lamellar steps, seen in all of the lamellar phases of this bolaamphiphile and shown schematically for the Lam-Nem in (d), are similar to the layer steps seen in FFTEM images of conventional smectics.

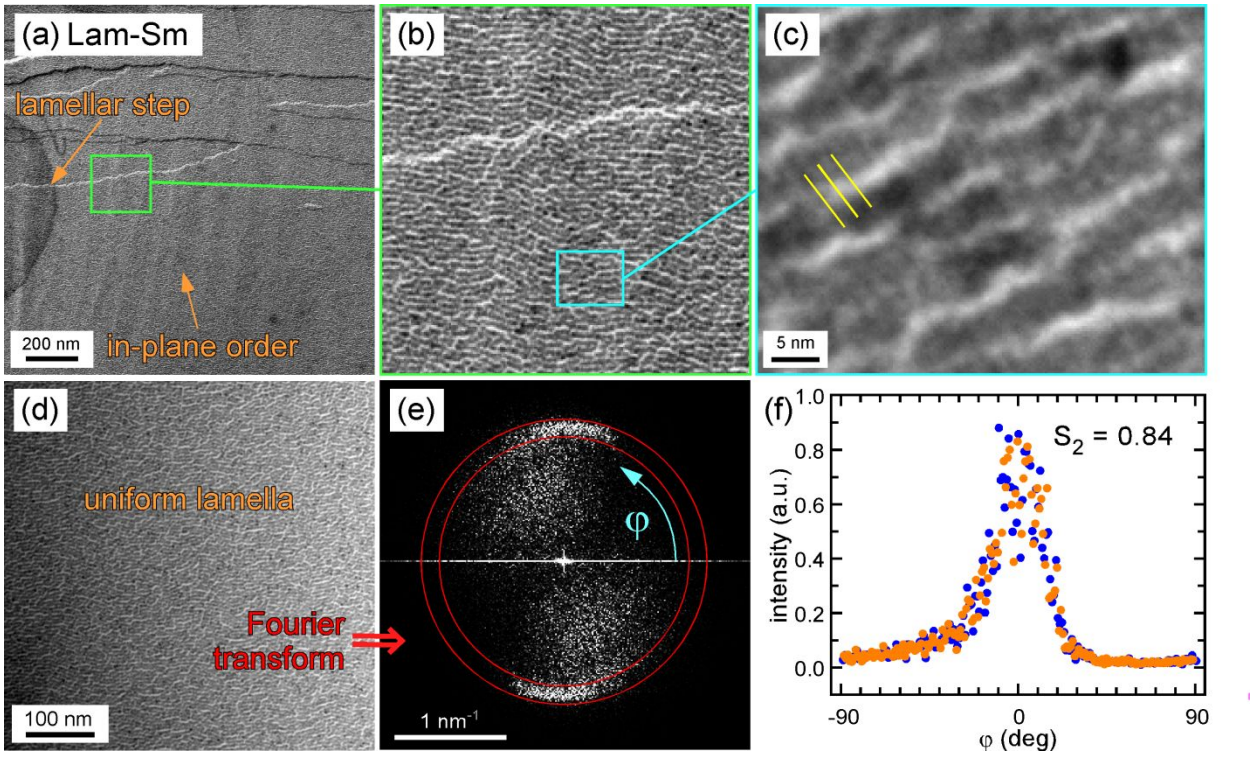

Figure 3: In-plane order of the Lam-Sm phase revealed by FFTEM. (a) FFTEM image of the Lam-Sm phase fractured in the bulk showing flat lamellae and lamellar steps. (b) An array of dislocated white stripes believed to be an artefact of the freeze-fracture process decorates the underlying texture of in-plane smectic layers formed by the rigid, rod-like, head cores. (c) At higher magnification, the in-plane smectic layers are visible as dark rows. The yellow lines are a guide to the eye showing the layer orientation. An image showing the white stripe texture in a region with homogeneous, in-plane smectic layering (d) may be Fourier transformed to obtain the equivalent of a scattering image (e). The diffraction peaks from the stripes (at around 1.2 nm^{-1}) are diffuse, with the red circles indicating the FWHM. Because of fluctuations of the stripe orientation, and hence of the smectic layer normal, the computed scattering is spread out in azimuth φ. (f) Combined computed scattering peaks (blue and orange dots), centered around φ =0. The orientational order parameter of the in-plane layer normal derived from the peak width is S_2=0.84.

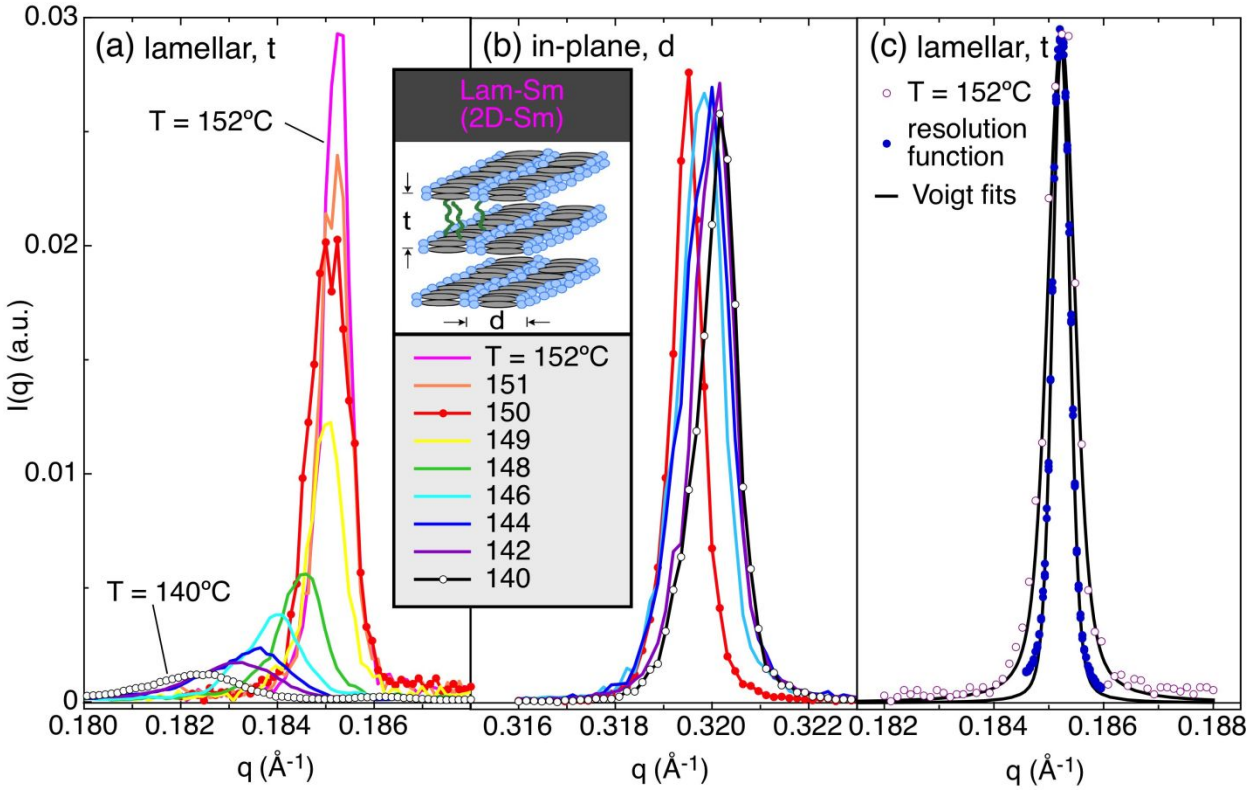

Figure 4: X-ray Bragg reflection peaks from randomly oriented bulk CT2 in a 1 mm diameter capillary. (a) Lamellar reflections in the temperature range 152ºC > T > 140ºC show peak broadening on cooling, indicative of the progressive loss of long-range, lamellar ordering in the Lam-Sm phase. (b) The in-plane (2D smectic) layering reflection is significantly wider than the instrumental resolution peak. (c) Example of lamellar reflection and diffractometer resolution peak fitted to Voigt lineshape functions. At high temperature (T τ152ºC), the lamellar peak is almost resolution-limited.

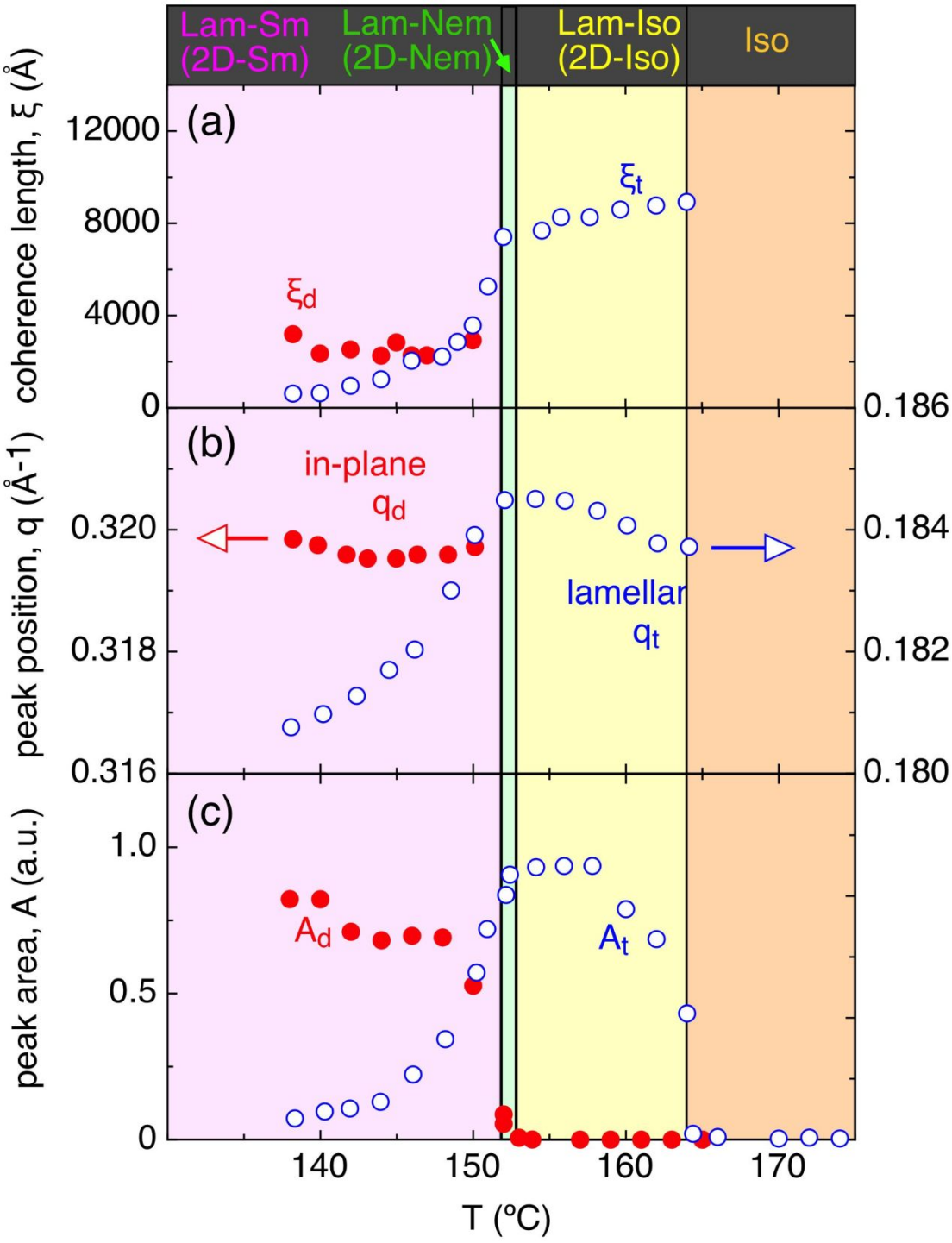

Figure 5: X-ray scattering parameters of CT2 as a function of temperature. The coherence lengths (a), peak positions (b), and integrated peak areas (c) are obtained by fitting the lamellar ("t") and in-plane ("d") x-ray reflections to Voigt lineshapes.

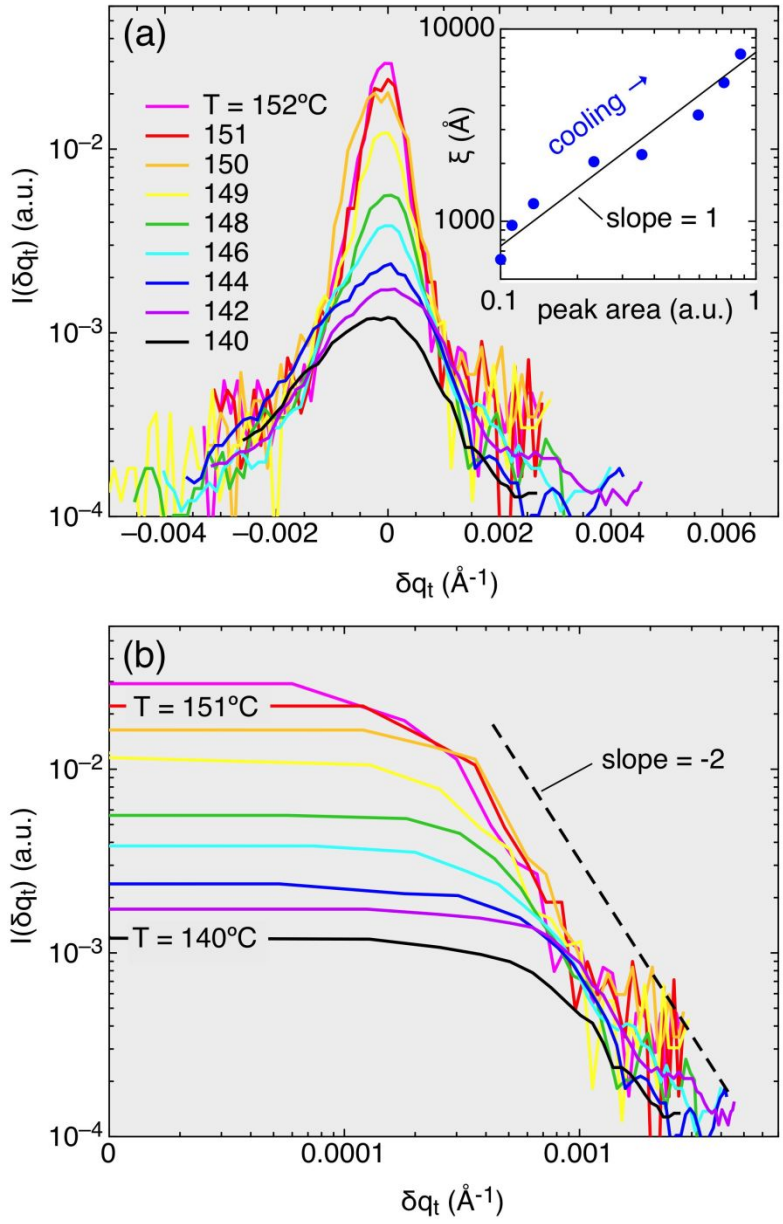

Figure 6: Lineshape analysis of lamellar x-ray diffraction peaks in the Lam-Sm phase. (a) Bulk lamellar x-ray diffraction peaks ($q_t \sim 0.18$ Å^{-1}) observed on cooling in the Lam-Sm phase, plotted vs. δq_t, the wavevector difference from the peak centroid. The tails overlap as is typically observed with a divergent susceptibility for smectic ordering. The inset shows that the correlation length and the integrated area of the lamellar reflection peak both increase on cooling as $\chi_o \propto 1/\xi^2$, typical 2nd-order critical behavior. (b)

Same lamellar scattering data as in (a), plotted on a log-log scale to emphasize the $1/\delta q_t^2$ dependence of the tails.

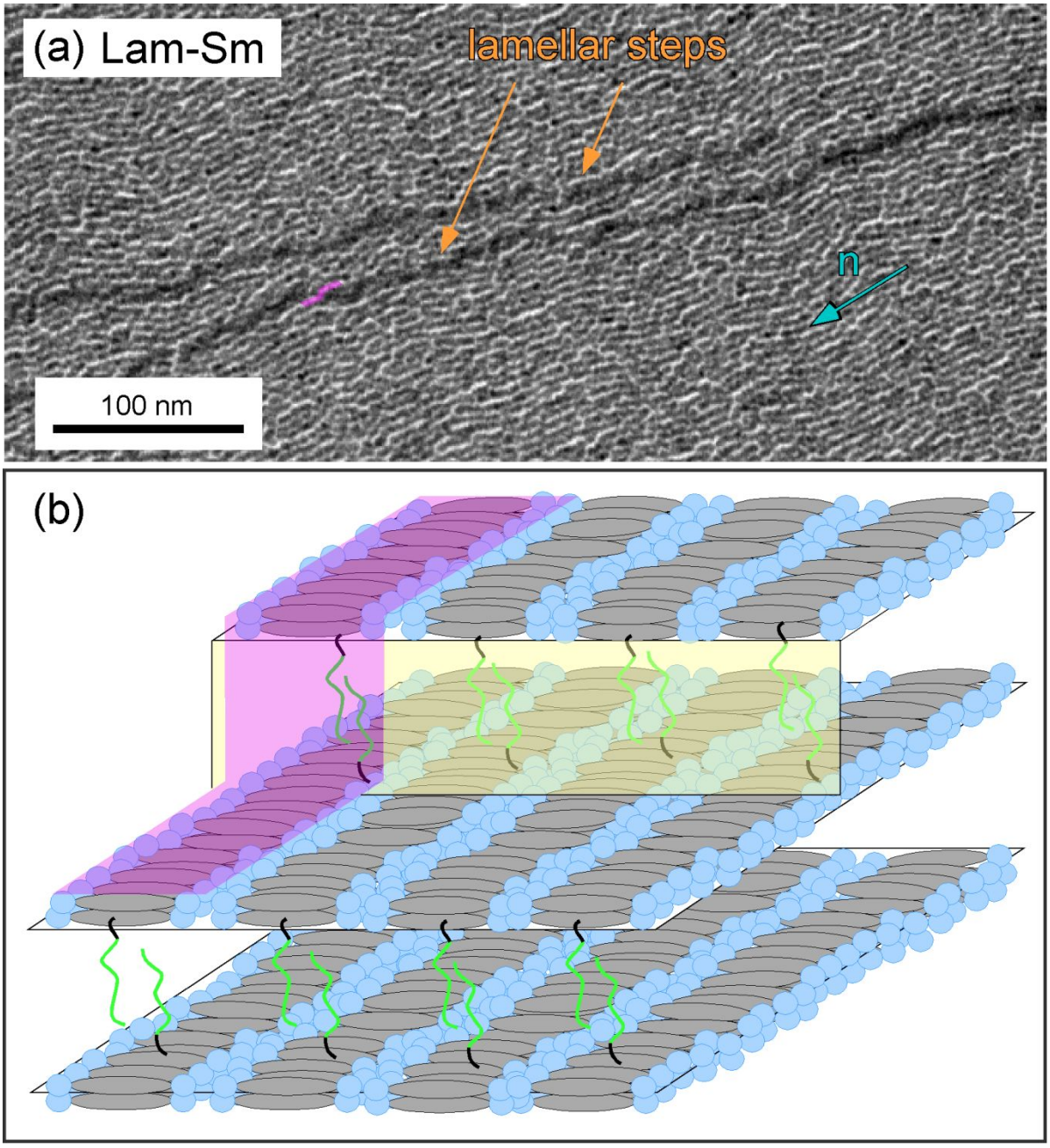

Figure 7: Interlayer correlation of the 2D smectic ordering. (a) FFTEM image of the Lam-Sm phase fractured in the bulk, showing locally periodic texture of the head groups (the local layer normal **n** is indicated by the blue arrow) and lamellar steps. The 2D smectic layers in neighboring lamellae have the same orientation, as evidenced by the continuity of the periodic

texture across the steps (an example is highlighted in magenta). (b) Schematic model of one of the lamellar steps in (a). The magenta shading emphasizes the continuity of the 2D smectic layers across the lamellae.

References

[1] Goodby JW, Collings PJ, Kato T, Tschierske C, Gleeson H, Raynes P, Vill V, Eds. Handbook of Liquid Crystals, Weinheim:Wiley-VCH; 2014. Vol 3 – 6.

[2] Kato T, Uchida J, Ichikawa T, Sakamoto T. Functional liquid crystals towards the next generation of materials. Angew. Chem. Int. Ed. 2018; 57:4355 – 4371.

[3] Goodby JW, Mehl GH, Saez IM, Tuffin RP, Mackenzie G, Auzély-Velty R, Benvegnu T and Plusquellec D. Liquid crystals with restricted molecular topologies: supermolecules and supramolecular assemblies. Chem. Commun. 1998; 998:2057 – 2070.

[4] Tschierske C. Development of structural complexity by liquid-crystal self-assembly. Angew. Chem. Int. Ed. 2013; 52B:8828 – 8878.

[5] Cheng XH, Das MK, Diele S, Tschierske C. Novel liquid-crystalline phases with layerlike organization. Angew. Chem., Int. Ed. 2002; 41:4031 – 4035.

[6] Tschierske C. Liquid crystal engineering – new complex mesophase structures and their relations to polymer morphologies, nanoscale patterning and crystal engineering. Chem. Soc. Rev. 2007; 36:1930 – 1970.

[7] Cheng XH, Das MK, Baumeister U, Diele S, Tschierske C. Liquid crystalline bolaamphiphiles with semiperfluorinated lateral chains: competition between layerlike and honeycomb-like organization. J. Am. Chem. Soc. 2004; 126:12930 – 12940.

[8] Prehm M, Enders C, Mang X, Zeng X, Liu F, Ungar G, Baumeister U, Tschierske C. Lamellar liquid crystals of in-plane lying rod-like mesogens with designer side-chains: the case of sliding versus locked layers. Chem. Eur. J. 2018; 24:16072 – 16084.

[9] Chattham N, Zhu C, Cheng X, Limtrakul J, Tschierske C, Maclennan JE, Clark NA. Direct observation of two-dimensional nematic and smectic ordering in freely suspended films of a bolaamphiphilic liquid crystal. Soft Matter. 2011; 7:9978 – 9982.

[10] Kosterlitz JM. The critical properties of the two-dimensional xy model. J. Phys. C: Solid State Phys. 1974; 7:1046 – 1060.

[11] De Gennes PG and Prost J. The Physics of Liquid Crystals. 2nd ed. Oxford: Clarendon Press; 1993.

[12] Van Winkle DH, Clark NA. Direct measurement of orientation correlations in a two-dimensional liquid-crystal system. Phys. Rev. A. 1988; 38:1573 – 1589.

[13] Nelson DR, Toner J. Bond-orientational order, dislocation loops, and melting of solids and smectic-A liquid crystals. Phys. Rev. B. 1981; 24:363 – 387.

[14] Patel NM, Dodge MR, Zhu MH, Petschek RG, Rosenblatt C, Prehm M, Tschierske C. Twist elasticity and anchoring in a lamellar nematic phase. Phys. Rev. Lett. 2004; 92:015501/1 – 4.

[15] Patel NM, Syed IM, Rosenblatt C, Prehm M, Tschierske C. Possible structures for the lamellar-isotropic (Lam-I) and lamellar-nematic (Lam-N) liquid crystalline phases. Liq. Cryst. 2005; 32:55 – 61.

[16] Chen D, Shen Y, Zhu C, Hough LE, Gimeno N, Glaser MA, Maclennan JE, Ros MB, Clark NA. Interface structure of the dark conglomerate liquid crystal phase. Soft Matter. 2011; 7:1879 – 1883.

[17] Stanley HE. Introduction to Phase Transitions and Critical Phenomena. Reprint edition. Oxford: Oxford University Press; 1987.

[18] Garland CW, Nounesis G. Critical behavior at nematic–smectic A phase transitions. Phys. Rev. E. 1995; 49:2964 – 2971.

[19] Bellini T, Radzihovsky L, Toner J, Clark NA. Universality and scaling in the disordering of a

smectic liquid crystal. Science. 2001; 294:1074 – 1079.

[20] Imry Y, Ma S. Random-field instability of the ordered state of continuous symmetry. Phys. Rev. Lett. 1975; 35:1399 – 1401.

[21] Golubović L, Lubensky TC, and O'Hern CS. Structural properties of the sliding columnar phase in layered liquid crystalline systems. Phys. Rev. E. 2000; 62:1069 – 1094.

[22] Rädler JO, Koltover I, Salditt T, Safinya CR. Structure of DNA – cationic liposome complexes: DNA intercalation in multilamellar membranes in distinct interhelical packing regimes. Science. 1997; 275:810 – 814.

[23] Salditt T, Koltover I, Rädler JO, and Safinya CR. Two-dimensional smectic ordering of linear DNA chains in self-assembled DNA-cationic liposome mixtures. Phys. Rev. Lett. 1997; 79:2582 – 2585.

[24] Tschierske C and Photinos DJ. Biaxial nematic phases. J. Mater. Chem. 2010; 20:4263 – 4294.